NANO · MICRO small

Supporting Information

for *Small*, DOI 10.1002/smll.202400303

Surfactant Micelle-Driven High-Efficiency and High-Resolution Length Separation of Carbon Nanotubes for Electronic Applications

Shuang Ling, Xiaojun Wei, Xin Luo, Xiao Li, Shilong Li, Feibing Xiong*, Weiya Zhou, Sishen Xie and Huaping Liu**

Supporting Information for

Surfactant Micelle-Driven High-Efficiency and High-Resolution Length Separation of Carbon Nanotubes for Electronic Applications

Shuang Ling,[1,2,6] Xiaojun Wei,[1,3,4,5,6,*] Xin Luo,[1] Xiao Li,[1,3,4] Shilong Li,[1,4] Feibing Xiong,[2,*] Weiya Zhou,[1,3,4,5] Sishen Xie,[1,3,4,5] and Huaping Liu[1,3,4,5,*]

[1] Beijing National Laboratory for Condensed Matter Physics, Institute of Physics, Chinese Academy of Sciences, Beijing 100190, China

[2] Department of Optoelectronic, Xiamen University of Technology, Xiamen, Fujian 361024, China

[3] Department of Physics and Center of Materials Science and Optoelectronics Engineering, University of Chinese Academy of Sciences, Beijing 100049, China

[4] Beijing Key Laboratory for Advanced Functional Materials and Structure Research, Beijing 100190, China

[5] Songshan Lake Materials Laboratory, Dongguan, Guangdong 523808, China

[6] These authors contributed equally

[*]Email: weixiaojun@iphy.ac.cn; fbxiong@xmut.edu.cn; liuhuaping@iphy.ac.cn

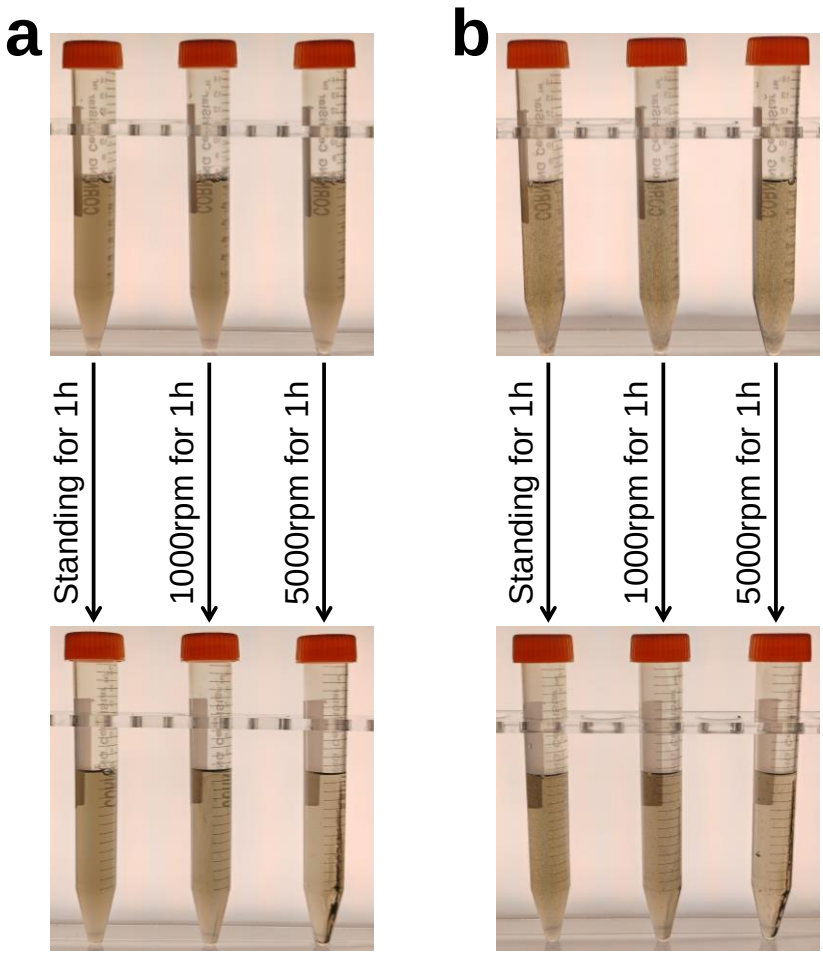

Figure S1. (a,b) Photographs of SWCNT dispersions in binary-surfactant system of 2% SDS + 0.2% SC after standing for 1 hour (left), and centrifugation treatments of 1000 rpm for 1 hour (middle) and 5000 rpm for 1 hour (right), in which the SWCNT dispersions with 0-hour (a) and 8-hour (b) standing were used as starting dispersions.

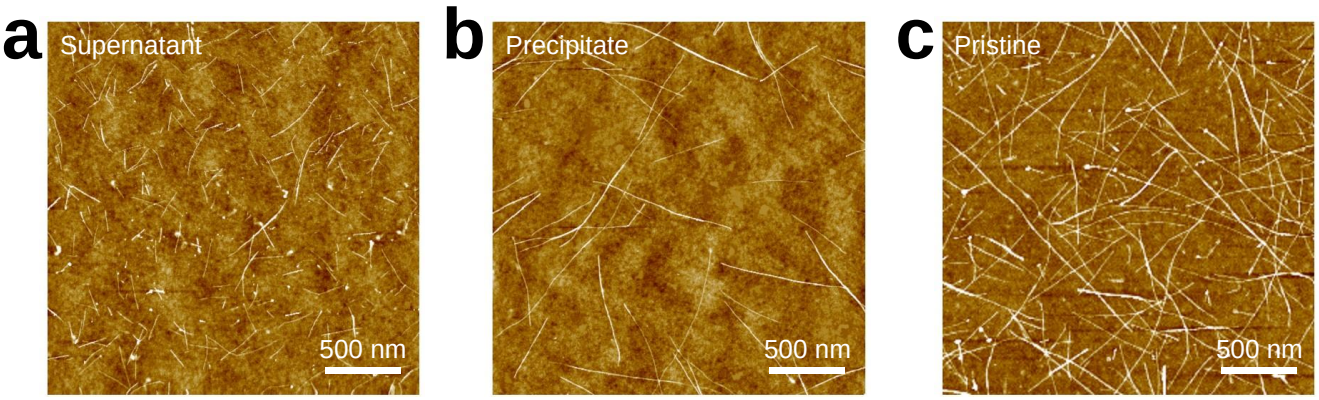

Figure S2. (a-c) Typical AFM images of the SWCNTs contained in the supernatant (a), precipitate (b), and pristine dispersion (c).

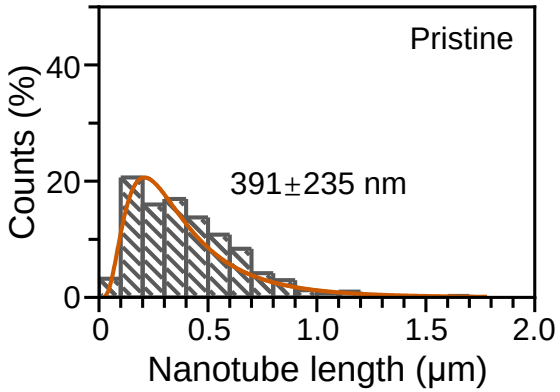

Figure S3. Length distribution of the pristine SWCNTs (before precipitation).

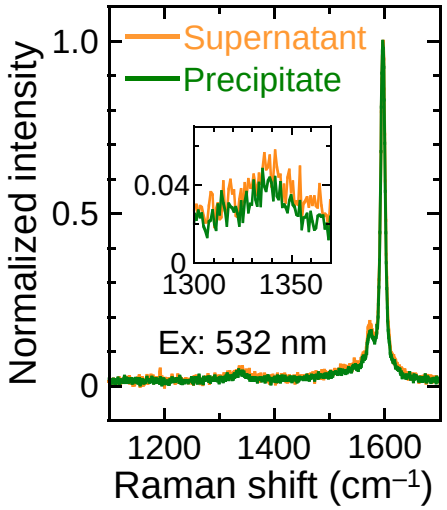

Figure S4. Raman spectra of SWCNTs contained in the supernatant and precipitate at an excitation wavelength of 532 nm, in which each spectrum was normalized by the maximum intensity of the G^+ band. Inset: enlarged spectra of the D mode region.

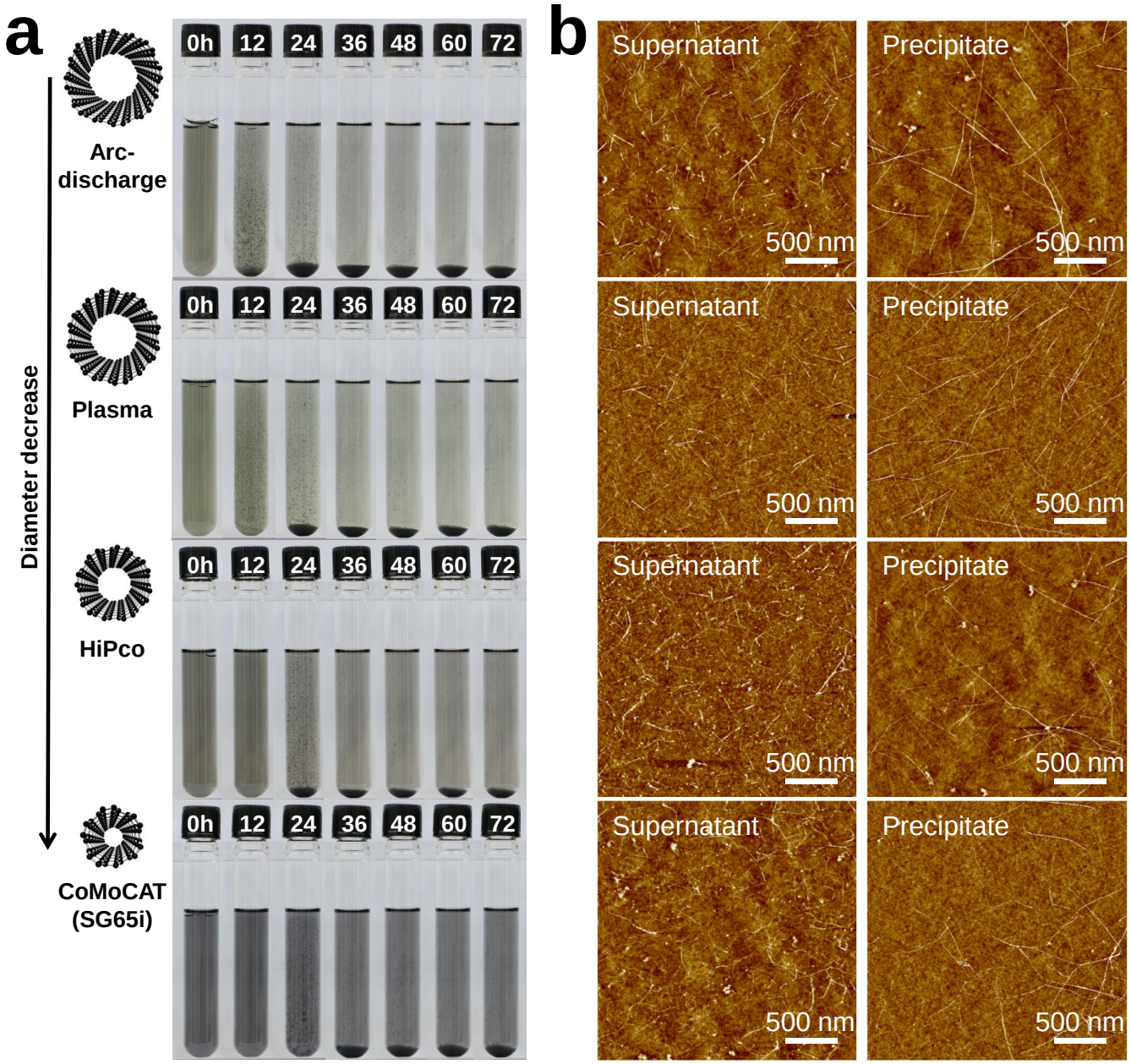

Figure S5. (a) Photographs of various SWCNT dispersions with different diameters after standing for various durations (0 − 72 hours), in which a binary-surfactant system of 2% SDS + 0.2% SC was used for each dispersion. (b) Typical AFM images of the SWCNTs contained in the supernatant and precipitate corresponding to (a).

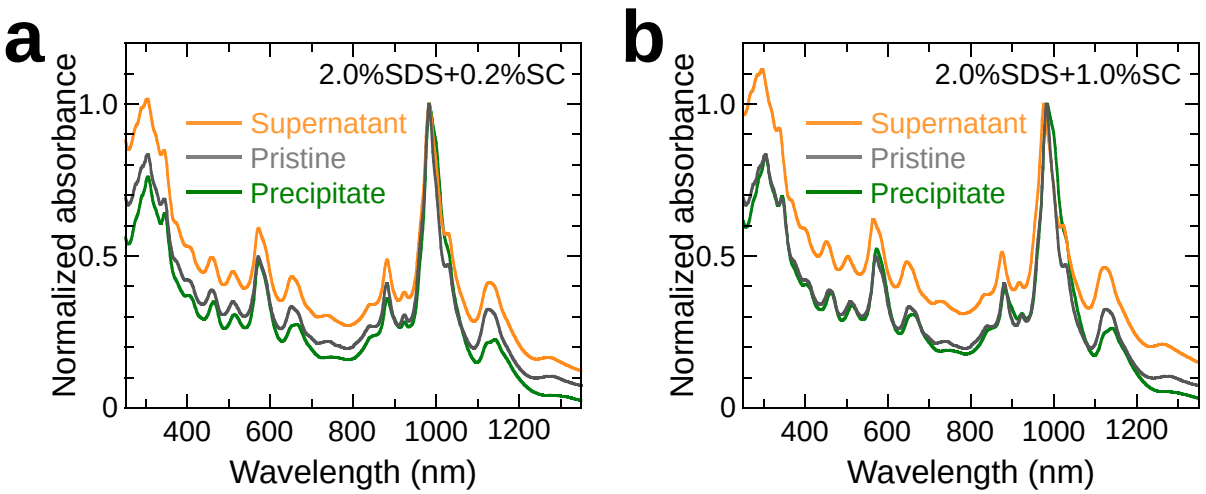

Figure S6. (a,b) Optical absorption spectra for the CoMoCAT SG65i SWCNTs contained in the supernatant and precipitate at 2.0% SDS + 0.2% SC (a) and 2.0% SDS + 1.0% SC (b), accompanied by optical absorption spectra of pristine CoMoCAT SG65i SWCNTs for comparison, in which each spectrum was normalized by the maximum absorbance in the S_{11} region.

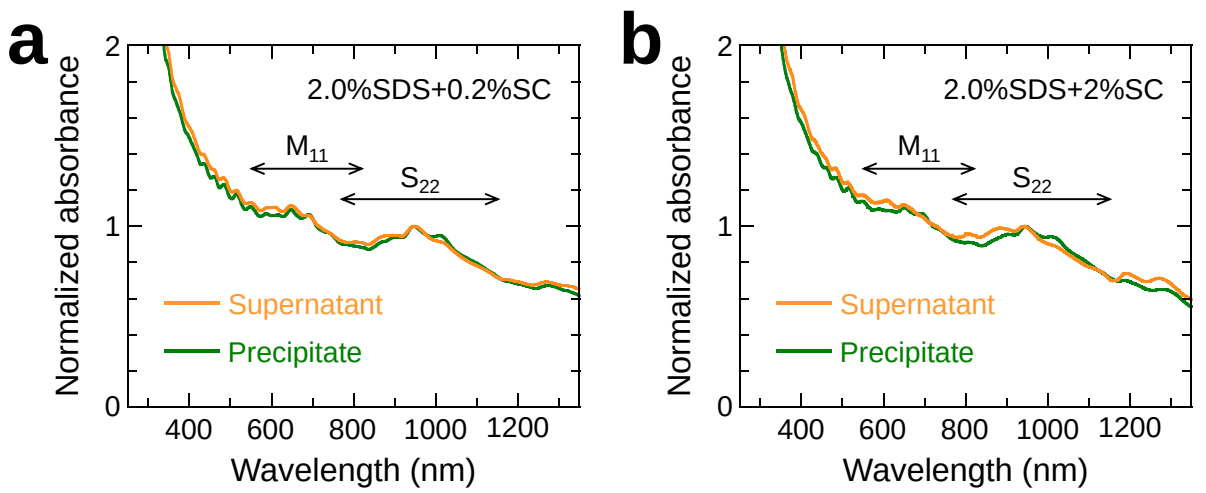

Figure S7. (a,b) Optical absorption spectra for the SWCNTs contained in the supernatant and precipitate at 2.0% SDS + 0.2% SC (a) and 2.0% SDS + 2.0% SC (b), in which each spectrum was normalized by the maximum absorbance in the S_{22} region.

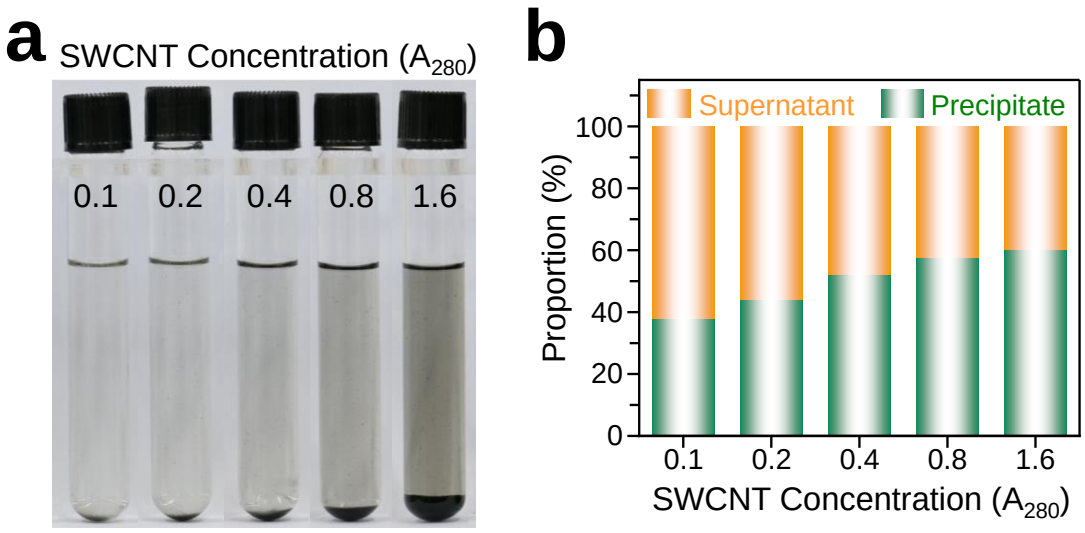

Figure S8. (a) Photographs of SWCNT dispersions with different SWCNT concentrations (A_{280}) after length-selective precipitation under the condition of 2% SDS + 0.2% SC. (b) Proportions of the supernatant and precipitate at different SWCNT concentrations (A_{280}).

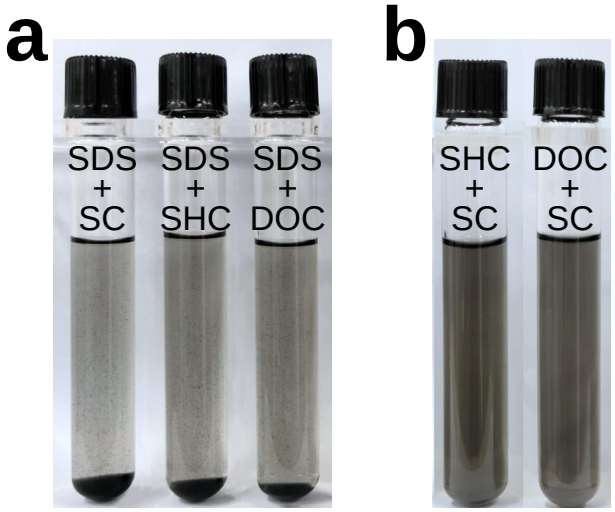

Figure S9. (a,b) Photographs of SWCNT dispersions after 48 hours of standing for a binary-surfactant system of 2% SDS + 0.2% SC (a, left), 2% SDS + 0.2% SHC (a, middle), 2% SDS + 0.2% DOC (a, right), 2% SHC + 0.2% SC (b, left), and 2% DOC + 0.2% SC (b, right), in which the SWCNT concentration was controlled the same for each dispersion.

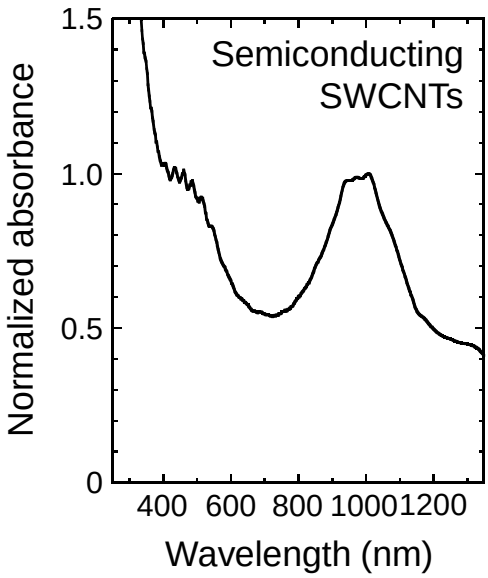

Figure S10. Optical absorption spectrum of the obtained semiconducting SWCNTs for length separation.

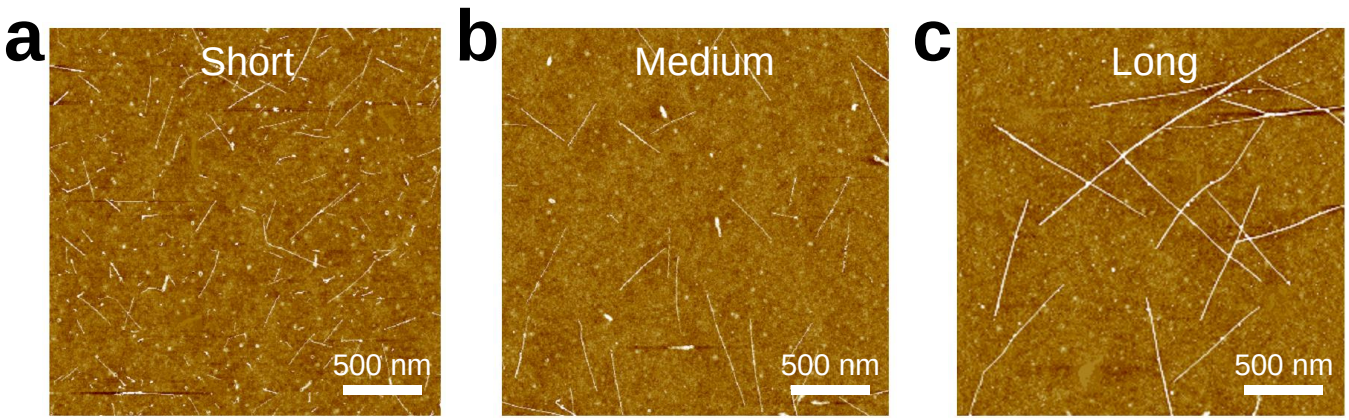

Figure S11. (a-c) Typical AFM images of short (a), medium (b), and long (c) SWCNTs obtained by the present two-step strategy.

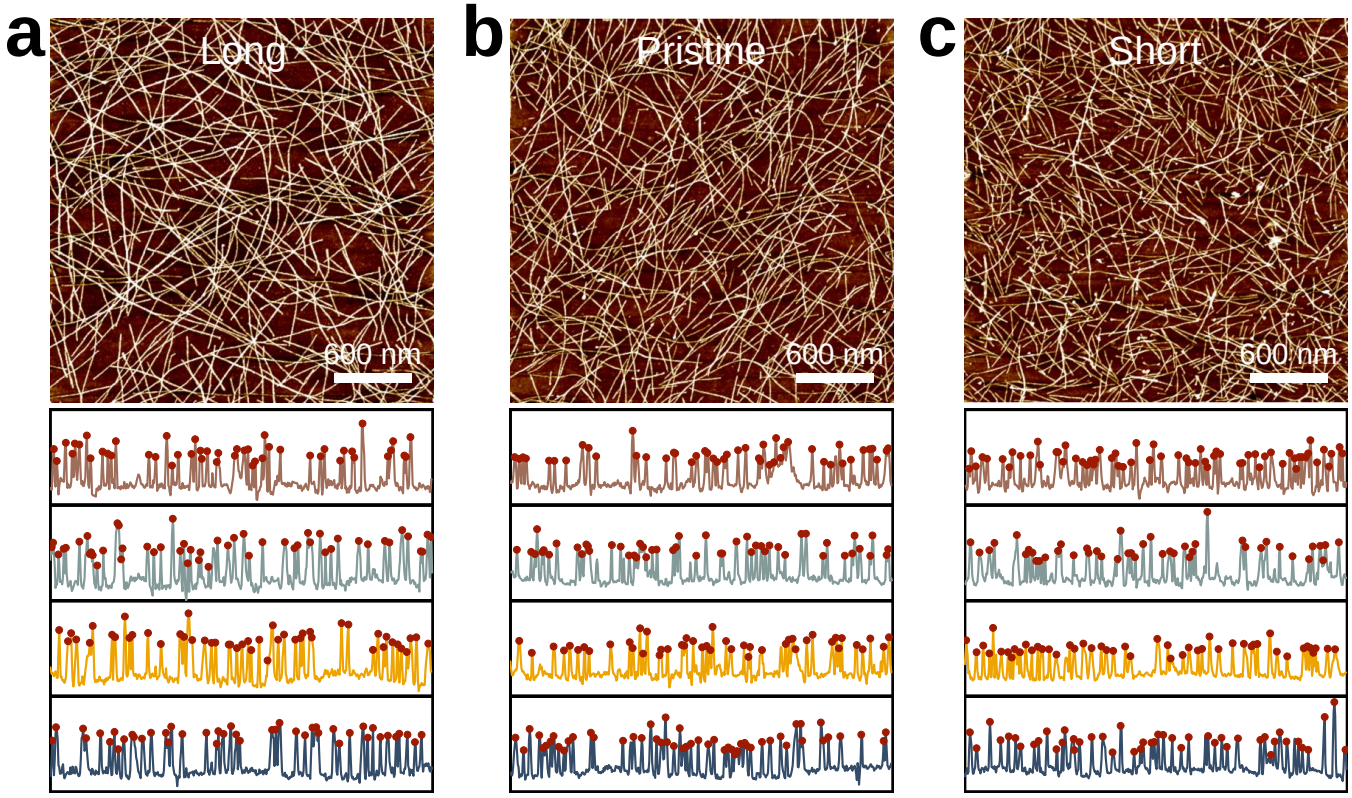

Figure S12. (a-c) Typical AFM images and corresponding linear density analysis for long (a), pristine (b), and short (c) semiconducting SWCNTs in the channel region. The linear densities were estimated to be approximately 16, 16, and 17 for long, pristine, and short semiconducting SWCNTs, respectively.

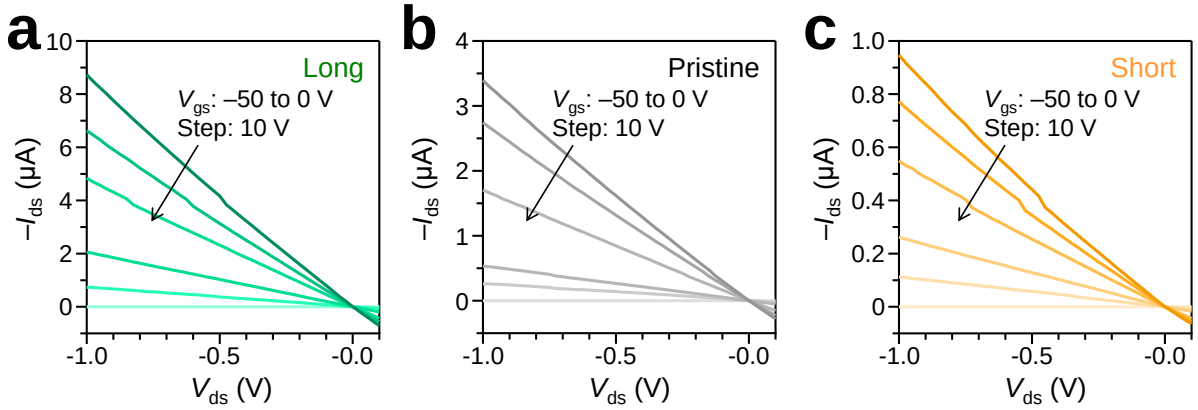

Figure S13. (a-c) Typical output characteristic curves of TFTs fabricated with long (a), pristine (b), and short (c) semiconducting SWCNTs at different V_{gs} voltages measured in vacuum, in which the curves at V_{gs} of –10 V were magnified 10, 50, and 10 times for long, pristine, and short semiconducting SWCNTs, respectively, for easy distinction.